Eur. Phys. J. Special Topics **191**, 3–14 (2010)

DOI: 10.1140/epjst/e2010-01338-4

THE EUROPEAN PHYSICAL JOURNAL SPECIAL TOPICS

Regular Article

Synchronization of slow-fast systems

I. Omelchenko, M. Rosenblum, and A. Pikovsky

Department of Physics and Astronomy, Potsdam University, Karl-Liebknecht-Str. 24-25, 14476 Potsdam, Germany

Received 22 November 2010 / Received in final form 23 December 2010
Published online 18 February 2011

Abstract. We describe different patterns of synchronization of two systems, each possessing oscillations on two very different time scales. Synchronization of slow and fast oscillations are characterized separately, leading to a possibility to observe partially synchronized states where, e.g., the slow motions are synchronous while the fast are desynchronized. As a first example we study two diffusively coupled Hindmarsh-Rose oscillators in the regime of regular or chaotic bursting and describe different synchronous states like phase synchronization of slow variables, burst and spike synchronization of fast variables, and complete synchronization. Next, we study two coupled four-dimensional model systems with chaotic slow dynamics and find phase synchronization of slow motion, complete and partially complete synchrony.

1 Introduction

Systems with a hierarchy of different time scales appear in many branches of natural sciences. In some cases, like in studies of fully developed hydrodynamic turbulence, such scales cannot be separated but form a cascade, what makes a description of the dynamics extremely difficult [1,2]. On the contrary, if well separated time scales can be attributed to particular variables, then a significant simplification of a system's complexity is possible. If the fast variables have simple dynamics, e.g., they just follow the slow ones, such a simplification can be efficiently achieved by virtue of the adiabatic elimination (also called slaving principle). In a more complicated case, when the fast variables exhibit a nontrivial dynamics, a simplified description is based on a method of averaging [3,4]. As examples of systems with distinct well separated slow and fast variables we mention lasers [5,6], chemical reactions [7], Josephson junctions [8–12], and Faraday ripples [13]. An example of particular interest is bursting neurons [14–19]. This regime of neuron operation, when epochs of quiescence intermingle with epochs of action potential (spike) generation, is quite common and important in neurodynamics. For example, there are evidences that in the hippocampus a relevant information is carried by the bursts rather than by single spikes. Neural bursting – with the spike patterns within a burst being either regular or irregular – is a representative example of the two-scale oscillatory dynamics [14–19].

In this paper we consider coupled multiple-scale systems, where fast variables have their own oscillatory dynamics. In these systems synchronization on slow and

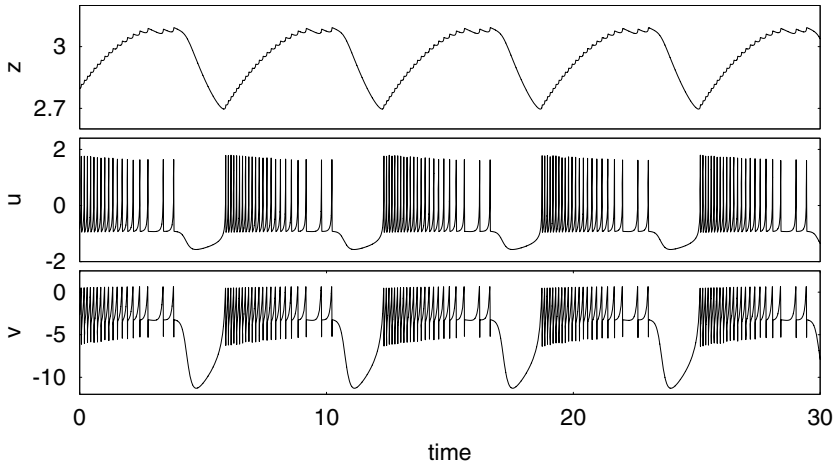

Fig. 1. Dynamics of the Hindmarsh-Rose system in the bursting regime. z is the slow variable and u and v are the fast ones. For parameters, see text.

fast time scales can be treated separately, and it is possible to observe synchronization effects in slow variables while the fast ones desynchronize.

2 Hindmarsh-Rose model and its dynamics

The main subject of our study in this paper is the Hindmarsh–Rose (HR) model [20], which is a reduced version of the celebrated Hodgkin-Huxley equations for modeling spike initiation in the squid giant axon [21]. The HR model describes the dynamics of the current through the neuron membrane and exhibits both periodic spiking and periodic or irregular bursting. The model has multiple time-scale dynamics [22–24] and its variables can be classified as fast and slow ones. The equations of the model are:

$$\frac{1}{\tau_s}\dot{z} = s(u + u_0) - z, \tag{1}$$

$$\frac{1}{\tau_f}\dot{u} = v - au^3 + bu^2 - z + J, \tag{2}$$

$$\frac{1}{\tau_f}\dot{v} = c - du^2 - v. \tag{3}$$

Here the variables u,v, and z represent the membrane potential of the neuron, the recovery variable, and the adaptation current, respectively. The current J represents an external influence on the system. Variable z is a slow one, whereas variables u and v are fast. We make this explicit by introducing a slow τ_s and a fast τ_f characteristic time scales into Eqs. (1)–(3). Respectively, in the following we refer to the first Eq. (1) as to a slow subsystem, and to two other equations (2)–(3) as to the fast subsystem. Because of the presence of the linear term u in the equation for z, the fast motion directly effects the slow one. For the first part of the paper (Secs. 3–6) we fix the parameter values as $s = 4$, $u_0 = 1.56$, $a = 1$, $b = 3$, $c = 1$, $d = 5$, and $J = 3$.

A typical dynamics of the HR system is illustrated in Fig. 1 for $\tau_s = 1$ and $\tau_f = 1000$. While the slow variable z demonstrates simple oscillations, the fast variables u and v demonstrate bursting: a sequence of spikes is followed by a quiescent

stage. Notice that the bursting and the quiescence occur at certain phases of the oscillation in the slow variable. The reason for such a dynamics is a bistability in the fast subsystem (2)–(3) if the slow variable z is considered as a fixed parameter (see Fig. 8 below). For some range of z the fast subsystem (2)–(3) possesses a stable limit cycle and a stable fixed point. In its slow dynamics the variable z oscillates, passing through the region of bistability of (2)–(3) back and forth, on one way via the limit cycle, and on the other way via the stable state, thus producing bursts.

3 Coupled Hindmarsh-Rose oscillators

In general, one says that a synchronization occurs when two oscillating systems having different natural frequencies adjust their rhythms due to a coupling. When applied to the multiscale dynamics like that of the HR model, this concept requires a careful definition of a natural frequency. As one can see from Eqs. (1)–(3), the time scales are defined by parameters $\tau_{s,f}$. In case of two coupled oscillators both the slow τ_s and the fast τ_f scales of two systems are generally different. Because we assume these differences to be relatively small, we define an "average" fast scale τ_f^0, so that for two systems with indices 1 and 2 we have $\tau_f^{1,2}/\tau_f^0 = 1 \mp \xi$ and $\tau_s^{1,2}/\tau_f^0 = \mu_{1,2} \ll 1$. In this way we separately describe the mismatch in the slow time scales by two parameters $\mu_{1,2}$, and the mismatch in the fast time scales by parameter ξ. By normalizing the time scale by τ_f^0 we obtain for the coupled systems:

$$\begin{aligned}
\dot{z}_{1,2} &= \mu_{1,2}[4(u_{1,2} + 1.56) - z_{1,2}], \\
\dot{u}_{1,2} &= (1 \mp \xi)(v_{1,2} - u_{1,2}^3 + 3u_{1,2}^2 - z_{1,2} + 3) + C(u_{2,1} - u_{1,2}), \\
\dot{v}_{1,2} &= (1 \mp \xi)(1 - 5u_{1,2}^2 - v_{1,2}).
\end{aligned} \tag{4}$$

Here we have introduced the coupling via fast variables u; C is the coupling factor. Throughout the first part of this paper we consider only coupling through the fast variables.

We notice that system (4) is a general model, with a simple diffusive coupling which may be considered as a simplified description of interaction between a pair of neurons via the gap junction. Although our study of the two-scale systems is motivated by neuronal dynamics, the primary goal of this paper is to analyze general synchronization properties of such systems. Therefore, we stay with the simple model (4) and refer to [25–31] for such different realistic aspects of burst synchronization as effects of the network topology, synaptic inhibitory or excitatory coupling, time delays, effects of noise, etc.

4 Types of synchronization

Analyzing system (4) we can speak of different levels of synchrony, according to which rhythms are adjusted. The rhythm of a slow variable z is naturally characterized by the period of its variation, or by its phase. The bursts of fast variables u and v are naturally characterized by the numbers of spikes in a burst. We denote this number as ν_k, where the index k numbers the bursts. Thus, each fast oscillator is quantified by a (regular or irregular) sequence of numbers $\nu_{1,2}(k)$. Basing on these notions, we focus on the following types of synchronization:

1. *Phase synchronization of slow variables.* The periods of slow variables z_1 and z_2 coincide and their phases are adjusted. This is the same notion of synchronization that is typically used for periodic and weakly chaotic oscillators [34].

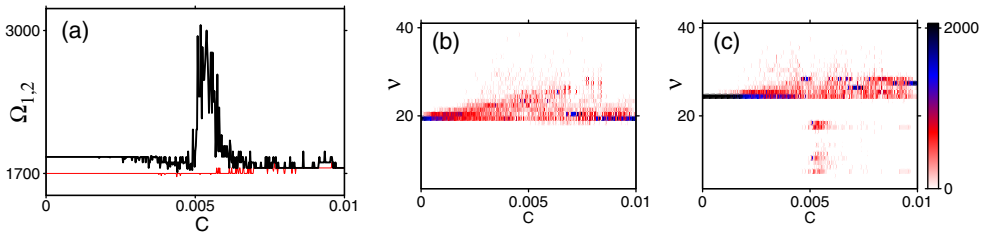

Fig. 2. (a) Frequencies of the first (thin line) and of the second (bold line) slow subsystems of Eqs. (4). (b), (c) Bursts diagrams for fast variables u_1 and u_2, respectively. Here the number of the bursts with a certain number of spikes ν are shown by gray scale coding (dark colors correspond to the most frequent values of ν). System parameters are: $\mu_1 = \mu_2 = 0.001$, $\xi = 0.15$.

2. *Burst synchronization of fast variables.* Here corresponding pairs of fast variables u_1 and u_2 (v_1 and v_2) exhibit bursts with equal numbers of spikes, i.e. $\nu_1(k) = \nu_2(k)$. Notice that it is not possible to characterize fast variables via phases since they are not defined during the quiescent stage.

   As illustrated by several examples below, phase synchronization of slow variables and burst synchronization of fast variables do not guarantee simultaneous spiking within each burst. Even if number of spikes are overall equal, spike patterns can be still asynchronous.
3. *Spike synchronization of fast variables.* Burst synchronization of fast variables with synchronous spike patterns.
4. *Complete synchronization*, i.e. a perfect coincidence of corresponding variables, implies combination of three criteria: phase synchronization of slow variables with zero phase shift, burst synchronization of fast variables, and simultaneous spiking within the bursts of fast variables.

Phase synchronization of slow variables without burst synchronization of fast variables can be also called as *partial* synchronization (we are indebted to P. S. Landa who first brought our attention to this regime). In the following two Sections we analyze these types of synchronization for coupled HR systems with different types of mismatch of their time scales.

5 Two coupled Hindmarsh-Rose neurons with matching slow scales

We set $\tau_s^1 = \tau_s^2$, what in terms of the rescaled system (4) means that the small parameters are equal, and $\mu_1 = \mu_2 = \mu$. For our simulations in this Section we fix parameter values $\mu = 0.001$ and $\xi = 0.15$, and vary the coupling in a range of small values $C \ll 1$.

First we focus on synchronization of slow variables. We calculated the frequencies $\Omega_{1,2}$ of $z_{1,2}$ by determining the number of oscillation periods over time interval $\Delta t = 10^5$, after discarding an initial transient of length $2 \cdot 10^5$. Figure 2(a) shows frequency graphs for slow variables z_1 (thin line) and z_2 (bold line). For very small coupling strength, C close to 0, slow variables demonstrate different frequencies: although the small parameter μ in both systems has the same value, they are not synchronized due to a mismatch in the fast subsystems. With increasing coupling strength, these frequencies become closer, and near the value $C \approx 0.007$ we observe synchrony on the slow time scale.

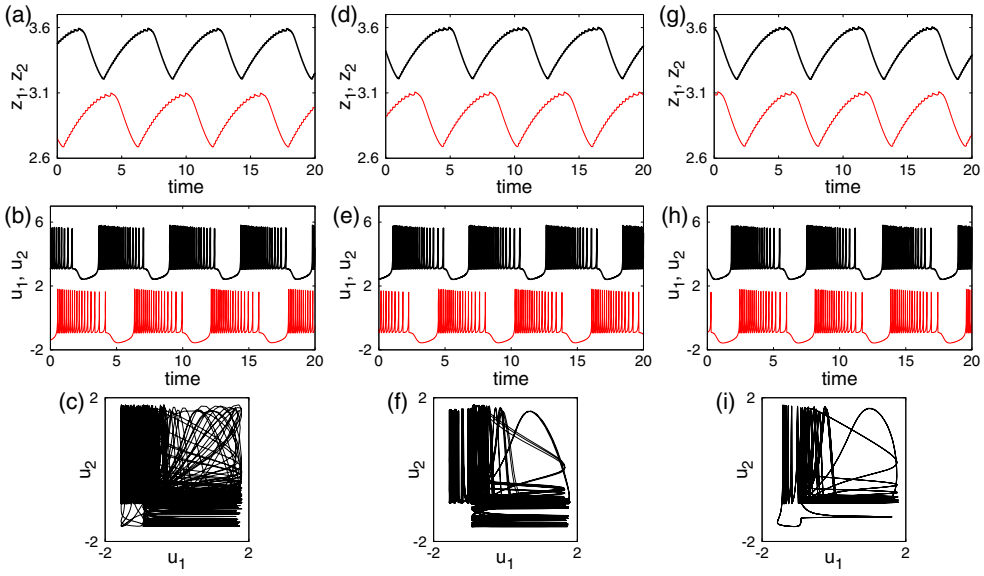

Fig. 3. Dynamics of slow variables (upper figures), fast variables and corresponding phase portraits for the system (4) with equal slow time scales. Values of coupling strength: (a), (b), (c) $C = 0.002$; (d), (e), (f) $C = 0.0055$; (g), (h), (i) $C = 0.009$.

Figures 2(b,c) demonstrate the bursts diagrams for fast variables u_1 and u_2. Namely, for the same time interval that was used in Fig. 2(a) for computation of $\Omega_{1,2}$ and the same transient time, the number of spikes ν_k in the series of bursts is plotted vs. the coupling strength C. More dark points correspond to the most frequent values of the number of spikes within the burst. We see that the most frequent values for the fast variables u_1 and u_2 are 20 and 22, respectively, in direct correspondence with the dynamics of uncoupled HR neurons with appropriate parameter values.

For very weak coupling, the numbers of spikes within the bursts are constant for each system, though this constants are different for two systems, and their slow variables are desynchronized. With increasing C, the coupling term effects the synchronization of slow variables, i.e. the number of bursts of two neurons within a long time interval becomes equal, while for the fast variables one observes bursts with different number of spikes ν. Obviously, they are close to their natural value 20 and 22, and their variations are not so large. Near the value $C = 0.005$ fast variable u_2 demonstrates series of bursts with a relatively small values of ν (from 7 to 18). This effects frequency of the slow variable z_2 (Fig. 2(a), bold line), which grows significantly in this range of the coupling strength. One can also give the following interpretation for the strong mismatch of slow frequencies for $C \approx 0.005$: Here one observes many "additional" bursts with a small number of spikes, thus the characteristic frequency of slow motion increases drastically.

Figure 3 demonstrates three typical examples of behavior for system (4) with equal slow time scales. In the plots Fig. 3(c,f,i) we characterize the synchrony *within* the bursts by plotting u_1 vs. u_2: if the plot is a closed curve, then the spikes in the bursts are synchronized, otherwise they are not. The first example ($C = 0.002$, left column) shows the situation where slow variables are desynchronized, so that the corresponding bursts of fast variables are also shifted in time, and phase portrait is an irregular trajectory. The second example ($C = 0.0055$, middle column) demonstrates the situation when the second subsystem produces spikes and bursts much faster then

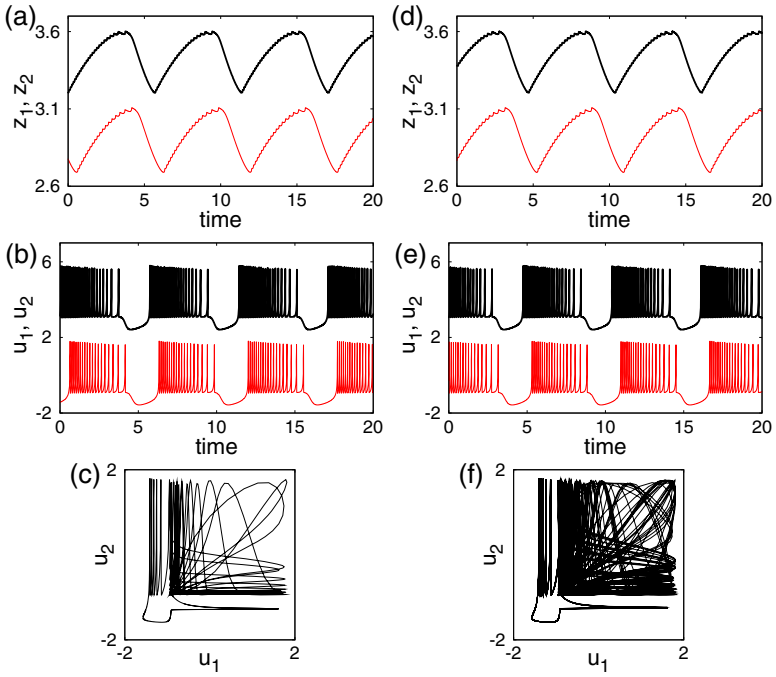

Fig. 4. Synchronization of two Hindmarsh-Rose neurons on slow time scale. (a), (b), (c) $C = 0.00725$, (d), (e), (f) $C = 0.0071$. (a), (d) Traces of slow variables z_1, z_2; (b), (e) traces of fast variables u_1, u_2; in each figure trace of the second neuron is shifted for better visualization. (c) Synchronous spiking (phase portrait in the plane (u_1, u_2)); (f) asynchronous spiking (phase portrait in the plane (u_1, u_2)). System parameters are: $\mu_1 = \mu_2 = 0.001,\ \xi = 0.15$.

the first one; in the phase plane we again observe an irregular trajectory. In the third example ($C = 0.009$, right column), slow variables are phase synchronized, and in the phase plane of fast variables we observe spike synchronization.

Synchrony in bursts can be accompanied by both regular or irregular patterns of spikes on the fast time scale. Figure 4 shows such patterns for parameter values $C = 0.00725$ and $C = 0.0071$, where synchrony on the slow time scale is observed. In the regular case (Fig. 4(a,b,c)) the motion is periodic and the bursts repeat one another up to individual spikes. In the irregular case (Fig. 4(d,e,f)) the spike pattern varies from burst to burst.

These variations can be weak, when the total number of spikes per burst is constant. If they are so large that the number of spikes changes from burst to burst than we do not observe burst synchrony of fast variables any more, and our system reaches regime of partial synchronization (this effect will be exemplified in the next Section).

6 Two coupled Hindmarsh-Rose neurons with different slow time scales

Here we consider two coupled HR neurons with different slow time scales $\tau_s^1 \neq \tau_s^2$, what in terms of the rescaled system (4) means that $\mu_1 \neq \mu_2$. For our simulations in this Section we fix parameter values $\mu_1 = 0.001$, $\mu_2 = 0.0013$, $\xi = 0.03$. The coupling strength C is varied in the interval [0,1].

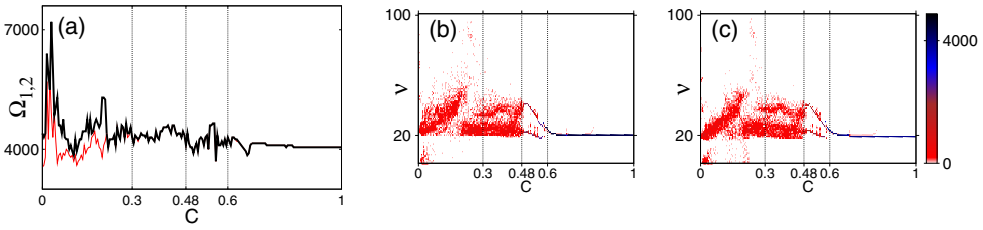

Fig. 5. (a) Frequencies of the first (thin line) and the second (bold line) slow subsystems. (b), (c) Distributions of the numbers of spikes in the bursts $\nu_{1,2}$ for fast variables u_1 and u_2; dark colors correspond to the most frequent values of ν. System parameters are: $\mu_1 = 0.001, \mu_2 = 0.0013$, $\xi = 0.03$.

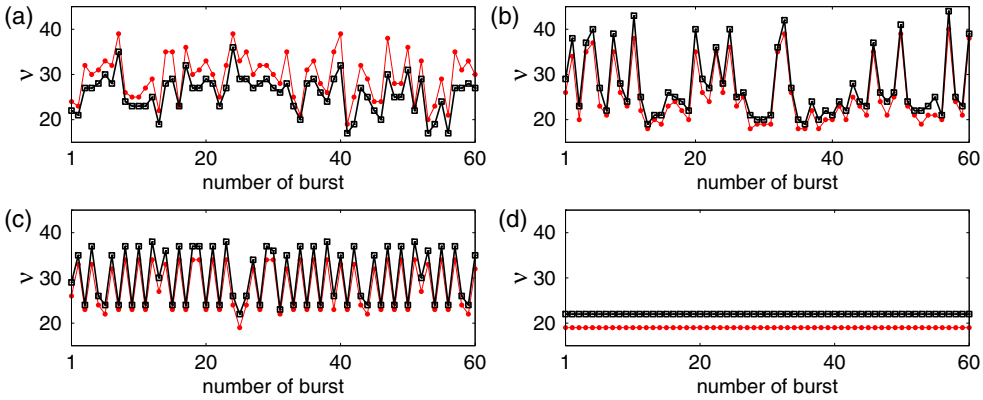

Fig. 6. Sequences of the number of spikes in bursts for fast variables u_1(thin) and u_2(bold). (a) $C = 0.1$, (b) $C = 0.4$, (c) $C = 0.55$, (d) $C = 0.9$. System parameters: $\mu_1 = 0.001, \mu_2 = 0.0013$, $\xi = 0.03$.

Figure 5 shows the frequency diagram for slow variables (Fig. 5(a)), and the corresponding burst diagrams for fast variables u_1 (Fig. 5(b)) and u_2 (Fig. 5(c)). From Fig. 5(a) we can see, that, contrary to the case $\mu_1 = \mu_2$, it is possible to achieve synchronization of slow variables for relatively strong coupling $C \approx 0.3$ only.

From Fig. 5 we can see, that system exhibits four qualitatively different dynamical regimes:

1. For small coupling $C \in (0, 0.3)$ slow variables are desynchronized, and fast variables demonstrate a wide range of values of the numbers of spikes ν in bursts;
2. For $C \in (0.3, 0.48)$ slow variables are phase synchronized, while the fast variables are still desynchronized and the values of $\nu_{1,2}$ are distributed in the range between 18 and 50;
3. For relatively strong coupling $C \in (0.48, 0.6)$ we observe phase synchronization of slow variables, while the fast variables now typically demonstrate series of alternating bursts, with two values of ν (with growth of C these two values become closer, and eventually come to values close to 20);
4. Finally, for very strong coupling $C \in (0.6, 1)$ slow and fast variables are synchronized, number of bursts as well as number of spikes in each burst are constant.

Figure 6 shows examples of the sequences of number of spikes in bursts for fast variables for four characteristic parameter regions described above (coupling strengths

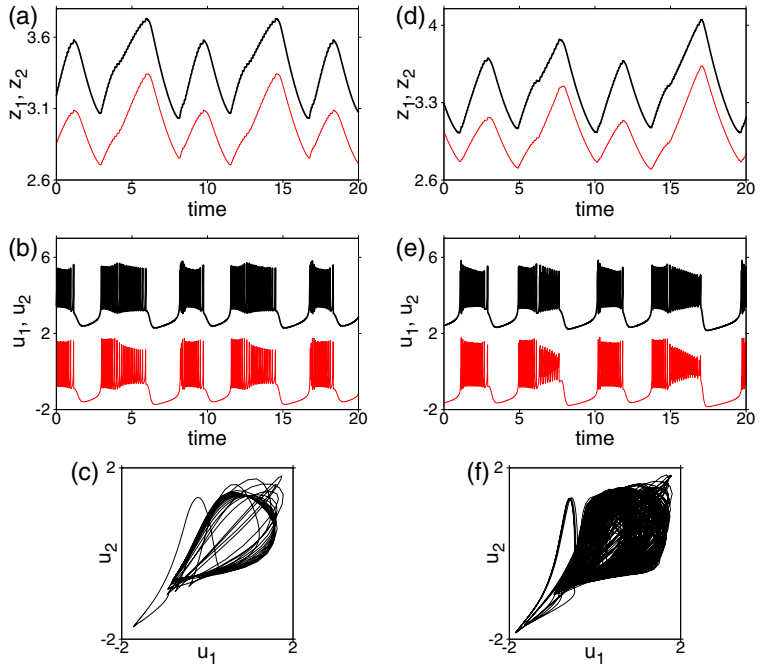

Fig. 7. Synchronization of two Hindmarsh-Rose neurons on slow time scale: (a), (b), (c) $C = 0.57$, (d), (e), (f) $C = 0.49$. (a), (d) traces of slow variables z_1, z_2; (b), (e) traces of fast variables u_1, u_2; in each figure trace of the second neuron is shifted for better visualization. (c) Synchronous spiking (phase portrait in the plane (u_1, u_2)); (f) asynchronous spiking (phase portrait in the plane (u_1, u_2)). System parameters: $\mu_1 = 0.001, \mu_2 = 0.0013$, $\xi = 0.03$.

$C = 0.1$, $C = 0.4$, $C = 0.55$, and $C = 0.9$). From this figure we can see, that in the case of small coupling, $C = 0.1$ (Fig. 6(a)), fast variables demonstrate different, although correlated numbers of spikes in the bursts. For relatively strong coupling, $C = 0.4$ (Fig. 6(b)), the numbers of spikes in each burst for the two fast variables u_1 and u_2 are close and strongly follow one another. At the same time, while these values differ from burst to burst, in the plane (u_1, u_2) we will observe a chaotic attractor. For $C = 0.55$ (Fig. 6(c)), the number of spikes oscillates between two values, and the dynamics of these oscillations for both fast variables is similar. Finally, for very strong coupling, $C = 0.9$ (Fig. 6(d)), fast variables u_1 and u_2 demonstrate stable synchronized behavior, producing identical bursts with 19 and 22 spikes correspondingly.

Thus, in the considered case $\mu_1 \neq \mu_2$, a rather strong coupling is required to synchronize slow dynamics. Nevertheless, such a synchronization is remarkable, because only fast variables are coupled. In the interval of couplings $C \in (0.3,\ 1)$, where the slow variables are synchronized, we observe complex, both regular or irregular patterns in bursts on the fast time scale. Figure 7 shows examples of such patterns for parameter values $C = 0.57$ and $C = 0.49$, where synchrony on the slow time scale is observed. In the first case (Fig. 7(a,b,c)) a pair of two different bursts is repeated and spike patterns overlap, being almost synchronized. In the irregular case (Fig. 7(d,e,f)) the spike patterns strongly vary from burst to burst and are desynchronized.

7 Synchronization of slow-fast systems with chaotic slow motions

In this Section we consider possible synchronization scenaria in the case when slow oscillations are *chaotic*. This is only possible if the slow dynamics is sufficiently

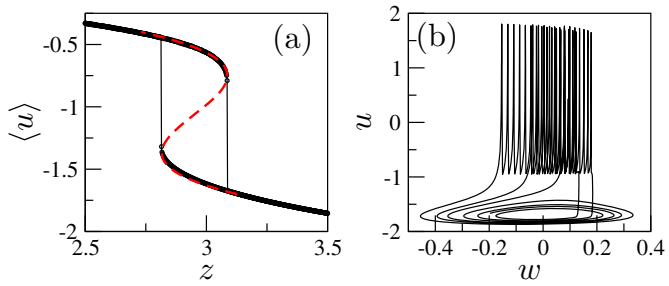

Fig. 8. (a) Dependence of $\langle u\rangle$ on z for the fast subsystem Eqs. (6). The upper and lower branches correspond to periodic motion and stationary state, respectively. Red dashed curve shows approximating cubic parabola. (b) Phase portrait of system (5,6) demonstrates chaos in slow motion for $J = -0.15$, $\mu = 0.005$. For better visualization only a short epoch with three bursts is depicted.

high-dimensional, so we extend the Hindmarsh-Rose model by one more slow variable w

$$\dot{z} = \mu[0.375z + w + 0.4(u + 1.7)], \qquad \dot{w} = -\mu z, \tag{5}$$

$$\dot{u} = v - u^3 + 3u^2 - z + J, \qquad \dot{v} = 1 - 5u^2 - v. \tag{6}$$

Here the value of the most parameters are the same as we used for the standard HR model (1–3). To analyze these equations we use a reduction based on the averaging over the fast time scale. As we know, in fast variables, for a fixed z and w, one either observes oscillations (a bursting state) or a steady state. In the former case we can average the variable u over the oscillation period, in the latter this average is simply the steady state value of u. As a result, we get a dependence $\langle u\rangle$ on z. It is more convenient to represent the inverse of this dependence as $z = F(\langle u\rangle)$. Numerics shows that it can be well approximated by a cubic parabola $F(x) = 0.94 - 7x - 7.33x^2 - 2.27x^3$ (see Fig. 8(a)). The property that $\langle u\rangle$ follows z can be formulated as a relaxation equation for this average

$$\frac{\mathrm{d}}{\mathrm{d}t}\langle u\rangle = \gamma[z - F(\langle u\rangle)], \tag{7}$$

where γ is a relaxation parameter of order of one (which has a meaning of the rate of attraction to a stable limit cycle or to the steady state in the fast subsystem, for a fixed z). Notice that although we cannot exactly determine this parameter, since we do not analyze relaxation properties of the fast subsystem thoroughly, the properties of the overall dynamics for $\mu \to 0$ are essentially independent of γ. Combining Eq. (7) with the equations for z, w we get a three-dimensional system

$$\dot{z} = \mu[0.375z + w + 0.4(\langle u\rangle + 1.7)], \tag{8}$$

$$\dot{w} = -\mu z\ , \qquad \langle\dot{u}\rangle = \gamma[z - F(\langle u\rangle)], \tag{9}$$

which has been investigated in [32,33] and is known to demonstrate chaotic behavior. In the limit $\mu \to 0$ its dynamics strongly depends on the value of μ, but is basically independent of parameter γ, the latter determines only how fast are the jumps between the stable branches of Fig. 8(a). Thus, the system (5,6) represents a slow-fast system with chaotic dynamics of the slow subsystem (Fig. 8(b)) and bistability "fixed point – limit cycle" in the fast subsystem. We illustrate chaotic slow-fast dynamics in Fig. 9.

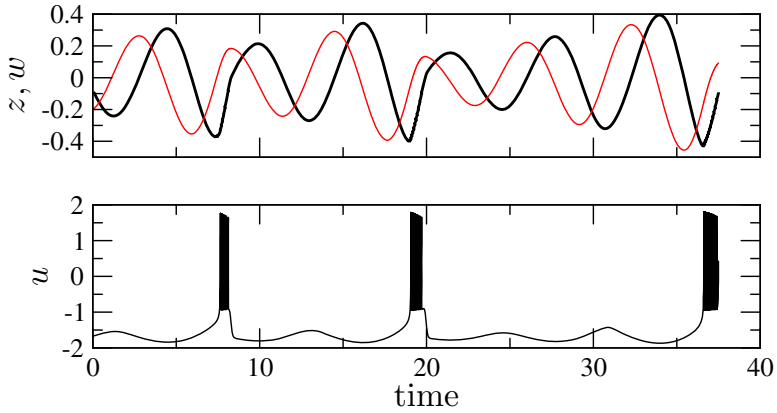

Fig. 9. Time series of slow (upper panel) and fast (bottom panel) motions in system (5,6). Bold and thin lines correspond to the variables z and w, respectively.

Next, we consider two systems with chaotic slow dynamics

$$\dot{z}_{1,2} = \mu_{1,2}[0.375z_{1,2} + w_{1,2} + 0.4(u_{1,2} + 1.7) + C(z_{2,1} - z_{1,2})], \tag{10}$$

$$\dot{w}_{1,2} = \mu_{1,2}(z_{1,2} + C(w_{2,1} - w_{1,2})), \tag{11}$$

$$\dot{u}_{1,2} = v_{1,2} - u_{1,2}^3 + 3u_{1,2}^2 - z_{1,2} + J, \qquad \dot{v}_{1,2} = 1 - 5u_{1,2}^2 - v_{1,2}, \tag{12}$$

linearly coupled via the slow variables, i.e.. via the terms $C(z_{2,1} - z_{1,2})$ and $C(w_{2,1} - w_{1,2})$. Parameters are $J = -0.15$, $\mu_1 = 0.001$, and $\mu_2 = 0.002$. The system are mismatched and in the absence of coupling we have two chaotic oscillators. Due to coupling they become adjusted, and as the first effect a phase synchrony between chaotic slow motions can be expected, followed by a more strong synchrony as the coupling increases.

In Fig. 10(a) we demonstrate phase synchronization of chaotic slow subsystems. This is essentially the same effect as the phase locking of periodic slow motions, discussed in Secs. 5,6, but for chaotic oscillators (see [34] for details). (Note that in the case considered in Sec. 6, slow motion becomes irregular due to the coupling, while here it is chaotic already in the uncoupled system.) Here the average frequencies $\Omega_{1,2}$ of slow oscillations become entrained already for small coupling, while these oscillations remain chaotic. For larger coupling the slow subsystems tend to complete synchronization, namely $\langle (z_1 - z_2)^2 \rangle$ and $\langle (w_1 - w_2)^2 \rangle$ decrease by three orders of magnitude (Fig. 10(b)). For coupling strength $C = 0.06$ the slow subsystems are very close to each other (Fig. 10(c)), although not fully identical due to difference in parameters $\mu_{1,2}$. In this regime the fast subsystems are very different (Fig. 10(d)). Therefore, this state can be characterized as a *partially complete synchronization*, because here slow subsystems are synchronized while the fast ones are not. For identical systems complete synchronization can set in for both slow and fast subsystems. So, in model (10–12) with $\mu_1 = \mu_2 = 0.001$ this happens for coupling $C_c \approx 0.05$, i.e. for $C > C_c$ both slow and fast variables in both subsystems are identical.

8 Conclusion

In this paper we studied synchronization effects in coupled systems demonstrating oscillations on two separate time scales. We have demonstrated that different

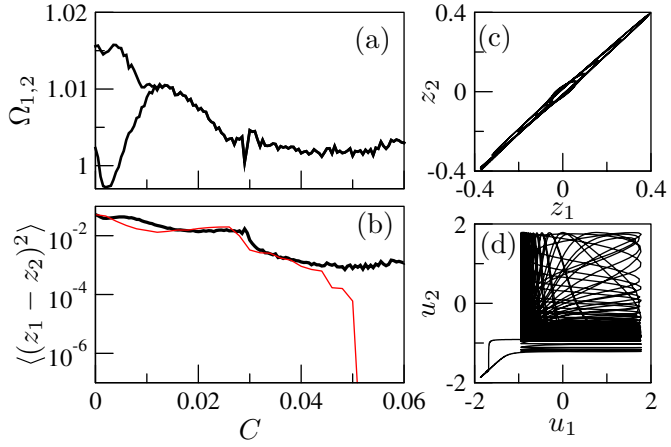

Fig. 10. (a) Phase synchronization of slow subsystems of Eqs. (10)–(12). (b) Complete synchronization of slow subsystems. Two cases are considered here. (i) $\mu_1 \neq \mu_2$. Here for large coupling the states of the slow variables are not identical, due to mismatch in μ, but the variance of $z_1 - z_2$ (bold line) and of $w_1 - w_2$ (practically coincide with the $z_1 - z_2$ curve and therefore not shown) essentially decrease with C. (ii) For identical systems, $\mu_1 = \mu_2$, a perfect complete synchronization sets in at $C \approx 0.05$, cf. [19] (solid line). (c,d) Complete synchronization of nonidentical systems for $C = 0.06$: slow variables nearly coincide whereas the fast variables remain asynchronous.

combinations of synchronization/desynchronization processes of slow and fast variables can be observed. In particular, partial synchronization, when slow subsystems synchronize (in the sense of complete or phase synchronization), whereas the fast subsystems can remain asynchronous or even become chaotic due to the coupling, has been described. We would like to stress that we focused here on a relatively simple case of a regular fast dynamics. The situation where fast motions in a single system are chaotic, requires a more elaborated analytical and numerical treatment, now in progress.

We thank P. S. Landa for illuminating discussions and DFG (SFB 555 “Complex Nonlinear Processes”) for support.

References

1. K. Fujimoto, K. Kaneko, Physica D **180**, 1 (2003)
2. A. Mazzino, S. Musacchio, A. Vulpiani, Phys. Rev. E **71**, 011113 (2005)
3. V.M. Volosov Uspehi, Math. Nauk **17**, 3 (1962), in Russian
4. N.N. Bogoliubov, Y.A. Mitropolsky, *Asymptotic Methods in the Theory of Nonlinear Oscillations* (Gordon and Breach, New York, 1961)
5. J.F.M. Avila, H.L.D.S. Cavalcante, J.R. Rios Leite, Phys. Rev. Lett. **93**, 144101 (2004)
6. I. Wedekind, U. Parlitz, Phys. Rev. E **66**, 026218 (2002)
7. S. Singh, J.M. Powers, S. Paolucci, J. Chem. Phys. **117**, 1482 (2002)
8. F.L. Vernon, R.J. Pedersen, J. Appl. Phys. **39**, 2661 (1968)
9. D.B. Sullivan, et al., J. Appl. Phys. **41**, 4865 (1970)
10. Y. Taur, P.L. Richards, J. Appl. Phys. **46**, 1793 (1975)
11. N. Calander, T. Claeson, S. Rudner, Appl. Phys. Lett. **39**, 504 (1981)
12. E. Neumann, A. Pikovsky, Eur. Phys. J. B **34**, 293 (2003)
13. M. Higuera, E. Knobloch, J.M. Vega, Theor. Comp. Fluid Dynamics **18**, 323 (2004)

14. E.A. Stern, D. Jaeger, C.J. Wilson, Nature **394**, 475 (1998)
15. R.C. Elson, et al., Phys. Rev. Lett. **81**, 5692 (1998)
16. P. Varona, et al., Biol. Cybern. **84**, 91 (2001), see also review by D. Golomb, D. Hansel, G. Mato, in *Neuro-informatics*, edited by F. Moss, S. Gielen (Elsevier, Amsterdam, 2001), vol. 4 of *Handbook of Biological Physics*, p. 887
17. M. Dhamala, V.K. Jirsa, M. Ding, Phys. Rev. Lett. **92**, 028101 (2004)
18. Y. Jiang, Phys. Rev. Lett. **93**, 229801 (2004)
19. A. Shilnikov, G. Cymbalyuk, Phys. Rev. Lett. **94**, 048101 (2005)
20. J.L. Hindmarsh, R.M. Rose, Proc. R. Soc. Lond. B **221**, 87 (1984)
21. A.L. Hodgkin, A.F. Huxley, J. Physiol. **117**, 500 (1952)
22. J. Guckenheimer, J. Tien, A. Willms, in *Bifurcations in the fast dynamics of neurons: implications for bursting, Bursting, The Genesis of Rhythm in the Nervous System,* edited by S. Coombes, P.C. Bressloff (World Scientific, 2005)
23. G. Innocenti, A. Morelli, R. Genesio, A. Torcini, Chaos **17**, 043128 (2007)
24. A.L. Shilnikov, M.L. Kolomiets, Tutorial. J. Bifurcations Chaos **18**, 1 (2008)
25. I. Belykh, E. de Lange, M. Hasler, Phys. Rev. Lett. **94**, 188101 (2005)
26. M.V. Ivanchenko, G.V. Osipov, V.D. Shalfeev, J. Kurths, Phys. Rev. Lett. **98**, 108101 (2007)
27. N. Burić, K. Todorović, N. Vasović, Phys. Rev. E **75**, 067204 (2007)
28. I. Belykh, A. Shilnikov, Phys. Rev. Lett. **101**, 078102 (2008)
29. N. Burić, K. Todorović, N. Vasović, Phys. Rev. E **78**, 036211 (2008)
30. X. Liang, M. Tang, M. Dhamala, Z. Liu, Phys. Rev. E **80**, 066202 (2009)
31. S. Jalil, I. Belykh, A. Shilnikov, Phys. Rev. E **81**, 045201 (2010)
32. S.V. Kijashko, A.S. Pikovsky, M.I. Rabinovich, Sov. J. Commun. Technol. Electronics **25** (1980)
33. A.S. Pikovsky, M.I. Rabinovich, Physica D **2**, 8 (1981)
34. A. Pikovsky, M. Rosenblum, J. Kurths, *Synchronization. A Universal Concept in Nonlinear Sciences* (Cambridge University Press, Cambridge, 2001)